THE JOURNAL OF BIOLOGICAL CHEMISTRY VOL. 287, NO. 8, pp. 5225–5234, February 17, 2012

Membrane Binding Events in the Initiation and Propagation Phases of Tissue Factor-initiated Zymogen Activation under Flow*

Received for publication, September 7, 2011, and in revised form, December 9, 2011 Published, JBC Papers in Press, December 20, 2011, DOI 10.1074/jbc.M111.302075

Laura M. Haynes[‡1], **Yves C. Dubief**[§], **and Kenneth G. Mann**[‡2]

From the [‡]*Department of Biochemistry, University of Vermont College of Medicine, Colchester, Vermont 05446 and the* [§]*Department of Mechanical Engineering, University of Vermont College of Engineering and Mathematical Sciences, Burlington, Vermont 05405*

Background: Much of our understanding of blood coagulation comes from "test tube" experiments that neglect the dynamics of the open vasculature.
Results: Membrane binding is critical in the activation of factor X under flow.
Conclusion: Different shear rates throughout the vasculature regulate factor Xa and thrombin presentation.
Significance: Determining flow's effects on coagulation will help us to understand differences between venous and arterial clots.

This study investigates the dynamics of zymogen activation when both extrinsic tenase and prothrombinase are assembled on an appropriate membrane. Although the activation of prothrombin by surface-localized prothrombinase is clearly mediated by flow-induced dilutional effects, we find that when factor X is activated in isolation by surface-localized extrinsic tenase, it exhibits characteristics of diffusion-mediated activation in which diffusion of substrate to the catalytically active region is rate-limiting. When prothrombin and factor X are activated coincident with each other, competition for available membrane binding sites masks the diffusion-limiting effects of factor X activation. To verify the role of membrane binding in the activation of factor X by extrinsic tenase under flow conditions, we demonstrate that bovine lactadherin competes for both factor X and Xa binding sites, limiting factor X activation and forcing the release of bound factor Xa from the membrane at a venous shear rate (100 s^{-1}). Finally, we present steady-state models of prothrombin and factor X activation under flow showing that zymogen and enzyme membrane binding events further regulate the coagulation process in an open system representative of the vasculature geometry.

The coagulation process is driven by the assembly of enzyme complexes on appropriate membranes (1). Tissue factor (TF)[3] released or exposed with vascular injury starts a sequence of membrane-dependent serine protease reactions culminating in the formation of a platelet-fibrin plug and hemorrhage control. Exposed membrane-associated TF forms a complex with circulating factor VIIa (fVIIa) to form the extrinsic tenase complex, which activates the zymogens fIX and fX to the active enzymes fIXa and fXa. The activation of fX to fXa is carried out ~100,000-fold more efficiently by the extrinsic tenase complex than by free fVIIa in solution (2–5). fXa in turn can activate catalytic amounts of the zymogen prothrombin (fII) to the active enzyme α-thrombin (fIIa), which activates the procofactor fV to the protein cofactor fVa. fVa and fXa assemble in the presence of Ca^{2+} on an appropriate phospholipid membrane to form the prothrombinase complex that is the primary source of fIIa with a 300,000-fold greater activity than free fXa in solution (6). The zymogens fII and fX bind to negatively charged phospholipids via Ca^{2+} mediated interactions with their γ-carboxyglutamate residues. It has been proposed that these membrane-localized fII and fX molecules can "skate" along the phospholipid membrane to come in contact with an appropriate membrane-isolated enzyme complex to be activated to their respective enzyme forms (7, 8). Although these reactions have been studied extensively under non-flow conditions, the influences of flow, such as would occur in the vasculature, on these reaction dynamics is less well characterized.

An important difference between closed "test tube" systems, in which substrates are distributed homogenously throughout a reaction mixture, and open flow systems, in which virgin substrate is continually resupplied, is that in the latter systems, the delivery of substrates to wall-bound enzyme complexes arises from the competition between flow transport, or flow convection, and the substrates' diffusion. The necessity to deliver substrate to wall-bound catalysts has the potential to introduce rate-limiting effects due to diffusional processes. Under this regime, potential substrate in the region of the catalytically active wall becomes depleted and effectively limits the rate of product formation. Conversely, if potential substrate is not depleted, then the major mediator of the enzymatic reaction is

* This work was supported, in whole or in part, by National Institutes of Health Grant P01 HL46703 (project 1) (to K. G. M.). This work was presented in part at the XXIII Congress of the International Society of Thrombosis and Haemostasis, Kyoto, Japan, July 25–29, 2011 (58).
This work is dedicated in memory of Drs. Yale Nemerson and Michael Nesheim.
[1] Supported by National Institutes of Health Thrombosis and Hemostasis Training Grant 5T32HL007594 (to K. G. M.).
[2] To whom correspondence should be addressed: Dept. of Biochemistry, 208 S. Park Dr., Colchester, VT. Tel.: 802-656-0335; Fax: 802-656-2256; E-mail: kenneth.mann@uvm.edu.
[3] The abbreviations used are: TF, tissue factor; f, factor; fII, prothrombin; fIIa, α-thrombin; h, human; b, bovine; r, recombinant; Φ, membrane binding site; PC, dioleoylphosphatidylcholine; PS, dioleoylphosphatidylserine; PCPS, dioleoylphosphatidylcholine/dioleoylphosphatidylserine; b-Lac, bovine lactadherin; HBS, HEPES-buffered saline; PEG, polyethylene glycol 8000; r.m.s., root mean square.

the flow rate through the catalytically active region. These two sets of conditions are termed "diffusion-mediated" and "dilution-mediated" control, respectively (9–12). Conditions favoring diffusion-mediated control include low flow rate, low substrate concentration, large cross-sectional tube dimensions, and low substrate diffusion coefficients. However, dilution-mediated control dominates when diffusion effects are minimized because the time scale of flow through the catalytically active region and the catalytic efficiency of the wall-localized enzyme do not permit sufficient depletion of substrate in the catalytically active wall region. Given the dynamic range of shear rates within the healthy vasculature ($\sim$50 s^{-1} in the inferior vena cava to 1900 s^{-1} in the arterioles) (13), as well as the disparities in coagulation proteins' physiologic concentrations, the interplay between diffusion- and dilution-mediated control requires consideration when interpreting how the coagulation process will perform in an open system.

Work from several groups has investigated how flow dynamics contribute to clot formation using whole blood- and plasma-based models (14–18). Additional computational modeling studies have also tried to determine the effects of flow on the biochemistry of blood coagulation under venous and arterial flow conditions (19–22). However, empirical flow studies detailing the dynamics of the individual coagulation reactions and their interactions with each other under flow conditions are scarce. To this end, the current study aims to determine the influence of flow on the activation of fX at both venous and arterial shear rates, both in isolation and with coincident fII activation by the prothrombinase complex.

We recently described (23) the activation of fII in an isolated system by the prothrombinase complex under a range of physiologic shear rates as being primarily regulated by flow-induced dilution and the mechanism of its activation as proceeding through a two-step mechanism in which the catalytically active intermediate meizothrombin may dissociate from one prothrombinase site before being fully activated to fIIa by a second prothrombinase complex. These results indicated that changes in the absolute concentration of fIIa generated do not vary with changes in shear rate and that the kinetics under relevant flow conditions do not vary from those that are observed in closed system experiments (23) and are in agreement with previous studies investigating the activation of fII under flow conditions (24–26). However, previous studies investigating the activation of fX by the extrinsic tenase complex under flow conditions have identified possible effects of diffusion on its activation at low shear rates, where the concentration of the fX substrate becomes significantly depleted close to the catalytically active wall (27). Furthermore, it has also been previously demonstrated in closed systems that competition between various protein species for membrane binding sites can dynamically influence coagulation reactions, including activation of fX by the extrinsic tenase complex (28–31).

Therefore, although the activations of both fX and fII under flow have been investigated previously (23–31), the aim of the present study is to understand how two activation processes functioning may influence each other under flow conditions. In the present study, we demonstrate that competition for available membrane binding sites (Φ) between two zymogens (fII and fX) and fXa capable of membrane binding will alter the presentations of both enzymes (fIIa and fXa) such that they deviate from pure diffusion- and dilution-mediated regimes observed when fX and fII are activated independently of each other under flow conditions. To further illustrate the importance of substrate binding to the membrane under flow conditions, we also present a model encompassing steady-state membrane binding and kinetics.

EXPERIMENTAL PROCEDURES

Materials—Synthetic phospholipid vesicles were prepared from 75% dioleoylphosphatidylcholine (PC) and 25% dioleoylphosphatidylserine (PS) (PCPS) or from 100% PC from Avanti Polar Lipids (Alabaster, AL) as described previously (32). Human fX (hfX), hfV, and hfII were purified as described previously (33, 34) or obtained as gifts from Hematologic Technologies (Essex Junction, VT). Human recombinant fVIIa (rfVIIa) and rTF(1–243) expressed in *Escherichia coli* were obtained as gifts from Dr. U. Hedner (Novo Nordisk) and Drs. S. L. Liu and R. Lundblad (Baxter Healthcare Corp., Durante, CA), respectively. rTF(1–243) was relipidated into PCPS or PC vesicles, lyophilized, and stored at −80 °C as described previously (35). Spectrozyme TH, Spectrozyme fXa, and hirudin were purchased from American Diagnostica (Stamford, CT). Bovine lactadherin (b-Lac) was received as a gift from Hematologic Technologies. αTF-5 and αTF-8 were received from the antibody core at the University of Vermont (Colchester, VT). hfIIa was prepared in house using a procedure modified from that of Lunblad *et al.* (36). hfV was activated to hfVa by incubating hfV (1 μM) with hfIIa (10 nM) in HEPES-buffered saline (HBS; 20 mM HEPES, 150 mM NaCl, pH 7.4) containing 0.1% polyethylene glycol 8000 (PEG) and 2 mM $CaCl_2$ for 20 min at 37 °C when hfIIa was inhibited by the addition of 12 nM hirudin. The concentration of hfVa was verified by its activity in hfV-deficient plasma in a prothrombin time clotting assay using TriniClot PT Excel S reagent (Trinity Biotech).

Preparation of Flow Chambers—Optically flat borosilicate glass capillaries (2 mm × 0.2 mm × 5 cm) from Vitrocom (Mountain Lakes, NJ) were prepared as described previously with slight modifications (23). Plasma-cleaned capillaries were filled with a solution containing PCPS or PC vesicles (100 μM) in the presence of relipidated rTF(1–243) (1 nM) in HBS containing 2 mM $CaCl_2$ and incubated for 1 h at 4 °C to assemble a supported phospholipid bilayer that incorporates rTF(1–243) (37, 38). Capillaries were rinsed with three volumes of HBS containing 2 mM $CaCl_2$ via capillary action and stored overnight in the same buffer. To assemble the extrinsic tenase complex, capillaries were incubated for 30 min to 1 h at 37 °C with rfVIIa (5 nM) in HBS containing 0.1% PEG and 2 mM $CaCl_2$. In coincident extrinsic tenase-prothrombinase experiments, hfVa (0.2 nM) was included in the rfVIIa coating solution. Prior to each experiment, the capillaries were rinsed with $\sim$200 μl (10 capillary volumes) of HBS containing 0.1% PEG and 2 mM $CaCl_2$ at a flow rate of 85 μl/min (shear rate $\sim$100 s^{-1}).

Flow Experiments—Experiments were conducted at 37 ± 3 °C. The flow apparatus is as described previously (23) with the exception that a second model 22 syringe pump (Harvard Apparatus, Holliston, MA) and four-way valve (GE Healthcare)

have been introduced to ease switching between different fluid mixtures. Reaction mixtures containing normal physiologic plasma concentrations of hfX (170 nM) with or without hfII (1.4 μM) in HBS containing 0.1% PEG and 2 mM $CaCl_2$ were flowed into capillaries containing preassembled extrinsic tenase with or without additional hfVa at shear rates between ~50 and 1000 ± 10% s^{-1} (flow rates 42.1–842 μl/min). The effluent was collected dropwise into a 96-well plate into HBS containing 0.1% PEG and 20 mM EDTA to stop further Ca^{2+}-dependent reactions. In coincident experiments, wells were alternately assayed for hfXa and thrombin; in wells to be assayed for hfXa activity, 50 nM hirudin was present in the quench solution. After each experiment, the capillary was rinsed for 5 min at a shear rate of 250 s^{-1} (flow rate = 213 μl/min) with HBS containing 0.1% PEG and 2 mM $CaCl_2$ and subsequently stripped with HBS containing 0.1% PEG, 20 mM EDTA, and 1% Triton X-100 (120 μl).

Assaying hfXa and Thrombin Activity—hfXa and thrombin activity were assessed for enzymatic activity against the chromogenic substrates Spectrozyme fXa and Spectrozyme TH (200 μM), respectively. Concentrations of hfXa and thrombin in the effluent were determined by comparison with a standard curve. The generation of hfXa and thrombin as a function of time were fitted to Equation 1 using the Graphpad Prism (version 5.02) software package as described previously, in which [*P*] is the concentration of product at any given time (*T*) or under final steady-state (*ss*) conditions, T_0 is the turning point of the function, and τ characterizes the rate of change upon approach to the final plateau.

$$[P(t)] = [P]_{ss} + \frac{[P]_{ss}}{(1 + T/T_0{}^{\tau})} \qquad \text{(Eq. 1)}$$

Bovine Lactadherin Competition for Membrane Binding Sites under Flow—The extrinsic tenase complex was assembled in PCPS/rTF(1–243)-coated capillaries as described above. hfX (170 nM) was flowed over the capillary at a shear rate of 100 s^{-1} until hfXa levels reached a steady state (~780 s) before b-Lac (20–200 nM) was added to the flowing solution. The change in hfXa generation ~780 s after the introduction of b-Lac was determined as a percentage of the steady-state levels of hfXa in the absence of b-Lac fit to Equation 1.

Measuring rTF(1–243) in Capillaries—rTF(1–243) was removed from capillaries by detergent extraction with Triton X-100. Its concentration in the extract was measured using a fluorescence-linked immunoassay as described previously in which rTF(1–243) was captured with αTF-5 and probed with αTF-48 (39, 40).

Closed Test Tube System Analyses of Extrinsic Tenase and Prothrombinase Kinetics—Closed test tube system kinetics for the activation of hfX by the extrinsic tenase complex were determined as follows: PCPS vesicles (100 μM), relipidated rTF(1–243) (100 pM), and rfVIIa (5 nM) were incubated for 10 min at 37 °C in HBS containing 0.1% PEG and 2 mM $CaCl_2$ to preassemble the extrinsic tenase complex. hfX (0.1–5 μM) was used to initiate the reaction from which samples were taken and quenched at 30-s intervals over a 5-min time course into HBS containing 0.1% PEG and 20 mM EDTA to stop Ca^{2+}-dependent reactions. hfXa concentrations were determined using Spectrozyme fXa (200 μM) and comparison with a standard curve. Closed test tube system kinetics for the prothrombinase complex were determined by incubating PCPS vesicles (20 μM), hfVa (20 nM), and hfXa (0.2 nM) for 5 min at 37 °C in HBS containing 0.1% PEG and 2 mM $CaCl_2$ to preassemble the prothrombinase complex. hfII (0.25–5 μM) was added to initiate the reaction. The reaction was sampled at 15-s intervals over a 2–3-min time course into HBS containing 0.1% PEG and 20 mM EDTA. hfIIa concentrations were determined using Spectrozyme TH (200 μM) and comparison with a standard curve.

Statistical Analyses—Statistical analyses were conducted using the Graphpad Prism (version 5.02) software package. The data were analyzed with one-way analysis of variance tests followed by Tukey's test.

THEORY

Estimating Degrees of Diffusion- and Dilution-mediated Control in Activation of fII and fXa over Range of Physiologically Relevant Shear Rates—The degrees of diffusion- and dilution-mediated control in the activations of fII and fX by wall-localized enzyme complexes can be estimated by applying the theories of Laidler and co-workers (9–12), which assume that there is sufficient enzyme on the surface of the capillary to convert as much substrate as encounters it. The interplay between flow-mediated dilution (convection) and diffusion-mediated reaction rates can be described by the Peclet number (P_e), which is the ratio of the rate of convection to the rate of diffusion of a single species. Bunting and Laidler (12) describe P_e as being proportional to the following term,

$$P_e \propto \left(\frac{DV}{v_F}\right)^{2/3} \cdot [S]_i \qquad \text{(Eq. 2)}$$

where *D* is the diffusion coefficient of the substrate, *V* is the volume of the tube, v_F is the average linear flow velocity, and $[S]_i$ is the initial substrate concentration. Under conditions where $[S_o]$ is much greater than the apparent K_m (Case A), the rate of the reaction to product, [*P*], is independent of the substrate concentration and is proportional to the inverse linear flow rate.

$$[P] \propto \left(\frac{1}{v_F}\right) \qquad \text{(Eq. 3)}$$

Conversely, when $[S_o] \ll K_m$, a diffusion-mediated effect will be observed (Case B) in which the activation of substrate to product is limited by the substrate's ability to diffuse to the catalytically active wall. Under these conditions, the concentration of product in the effluent is proportional to the inverse cubed root of the linear flow rate.

$$[P] \propto \left(\frac{1}{v_F}\right)^{1/3} \qquad \text{(Eq. 4)}$$

The degree of diffusional control can therefore be assessed by a double-logarithmic plot of linear velocity *versus* the concentration of product in the effluent. A slope of −1 would indicate conditions favoring Case A, whereas a slope of −2/3 would indicate conditions favoring Case B.

Steady-state Levels of Membrane-bound Components—The concentrations of the three substrates and products capable of membrane binding in our studies (fII, fX, and fXa) can be described by their dissociation constants (K_d) as follows, where f and b denote free and bound species, respectively, and Φ denotes binding sites.

$$K_{d,fII} = \frac{[fII]_f[\Phi]_f}{[fII]_b} \quad \text{(Eq. 5)}$$

$$K_{d,fX} = \frac{[fX]_f[\Phi]_f}{[fX]_b} \quad \text{(Eq. 6)}$$

$$K_{d,fXa} = \frac{[fXa]_f[\Phi]_f}{[fXa]_b} \quad \text{(Eq. 7)}$$

Literature K_d values are listed in Table 1. At the steady state, the concentrations of the relevant species are described as follows, where t denotes total and i denotes the initial concentrations of the relevant species.

$$[fX]_f = [fX]_i - [fX]_b - [fXa]_t \quad \text{(Eq. 8)}$$

$$[fII]_f = [fII]_i - [fII]_b - [fIIa] \quad \text{(Eq. 9)}$$

$$[fXa]_t = [fXa]_f + [fXa]_b \quad \text{(Eq. 10)}$$

The total number of binding sites was determined by taking the surface area of the capillary (2.2 cm^2) and assuming that a single phospholipid headgroup occupies an area of 75 $Å^2$ (41). We assume that the presence of enzyme complexes on the membrane is negligible in calculations of available binding sites (8, 42, 43). Assuming that fII, fX, and fXa occupy binding sites consisting of 50 phospholipid headgroups, we estimate that there are ~9.7 pmol of available binding sites, $[\Phi]_i$ within the total volume of the capillary. We describe the total concentration of free binding sites as follows.

$$[\Phi]_f = [\Phi]_i - [fII]_b - [fX]_b - [fXa]_b \quad \text{(Eq. 11)}$$

Although the reactions are occurring in a two-dimensional space on the surface of the capillary, we treat the vertical component of the volume element as the average root mean square (r.m.s.) diffusion distance of fII, fX, and fXa at 37 °C in the average time it takes one capillary volume to flow through the capillary at a given shear rate (Table 2). We validate this approximation of the volume element by comparing the r.m.s. diffusion distances with the distances of greatest thrombin flux, which we previously reported as a function of shear and are consistent with the current approximations (23). The average r.m.s diffusion distance of the three species was determined and treated as the half-height of the capillary (H, 100 μm) to estimate the concentration of relevant species confined to an appropriately sized region close to the capillary wall. We term the inverse of this fraction the spatial confinement factor (ξ). Under these conditions of spatial confinement, the populations of bound and free species were calculated using the assumption that the measured fIIa and fXa levels in the effluent correspond to unbound species.

Modeling Kinetics of fII and fX Activation under Laminar Flow Conditions—The kinetics of fII and fX activation were simulated under two extreme regimes: 1) conditions under which the zymogen activation is driven by diffusion of substrates from the bulk to the catalytically active wall region,

$$V_{max} = \frac{k_{cat}[E][S]_t}{K_M + [S]_t} \cdot \xi \quad \text{(Eq. 12)}$$

and 2) conditions under which zymogen activation is dominated by membrane localized events.

$$V_{max} = \frac{k_{cat}[E]_b[S]_b}{K_m + [S]_b} \cdot \frac{1}{F_m} \quad \text{(Eq. 13)}$$

K_m and k_{cat} are the relevant kinetic constants, $[E]$ is the effective concentration of membrane-localized enzyme in the confined volume at a given shear rate, $[S]_t$ is the total concentration of free and bound substrate in the vicinity of the phospholipid membrane at a given shear rate, $[E]_b$ and $[S]_b$ are the concentrations of membrane-localized enzyme and substrate in a unit volume of 100 Å above the capillary wall (approximately the height of the extrinsic tenase and prothrombinase active site from an appropriate membrane), and F_m is the membrane confinement factor (here equal to a 10,000-fold increase in concentration from that in the total capillary volume). Similar kinetic schemes have been employed previously to describe the activation of fII by prothrombinase on phospholipid vesicles (7, 44). The concentrations of fIIa and fXa were determined by multiplying V_{max} by the average time it takes one capillary volume to pass through at a given shear rate.

TABLE 1
Dissociation constants (K_d) and diffusion coefficients ($D_{37,w}$) of relevant species

Species	K_d	$D_{37,w}$
	nM	$s\,cm^{-2} \times 10^7$
fII	230 (54)	7.67 (55)
fX	250 (54)	8.59 (56)
fXa	114 (8)	11.5 (57)

RESULTS

Surface Densities of Enzyme Complexes—The results of the TF immunoassay (n = 19), showed that the surface density of rTF(1–243) to be 2.2 ± 0.5 fmol cm^{-2} (~26 molecules/μm^2) for the capillaries used in both the isolated extrinsic tenase

TABLE 2
r.m.s. diffusion distances of relevant proteins

Shear	fII	fX	fXa	Average r.m.s. distance	Species confinement factor (ξ)
s^{-1}	μm	μm	μm	μm	μm
50	66.1	70.0	81.0	72.3	1.39
100	46.5	49.2	57.0	50.9	1.98
250	29.3	31.0	35.9	32.1	3.14
1000	14.7	15.5	17.9	16.0	6.28

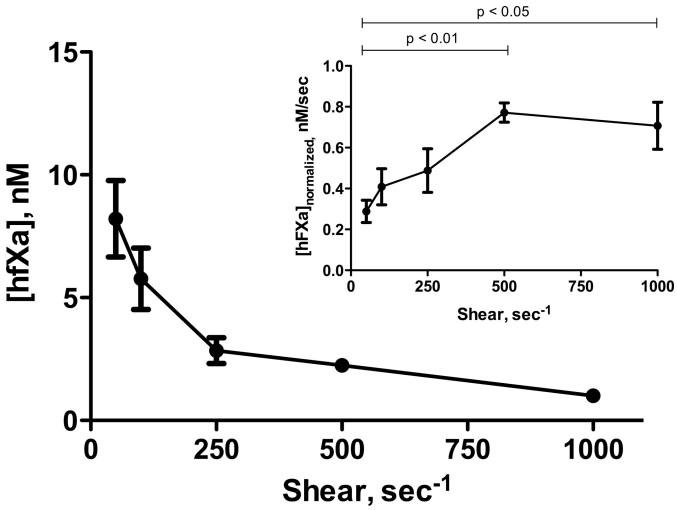

FIGURE 1. **Activation of hfX by extrinsic tenase under flow conditions.** hfX at a physiologic plasma concentration (170 nM) was flowed over PCPS-coated glass capillaries in which the extrinsic tenase complex was assembled over a range of physiologically relevant shear rates (50–1000 s^{-1}). The effluent was collected dropwise and assayed for hfXa activity. Absolute steady-state levels of hfXa ($n = 4$) are reported as well as mean ± S.D. (*error bars*) as a function of shear rate. Average capillary passage time-normalized levels of hfXa generation are shown in the *inset*. Normalized hfXa levels at 50 s^{-1} are significantly different from those measured at 500 and 1000 s^{-1}.

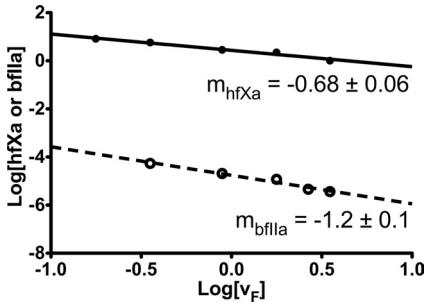

FIGURE 2. **Determination of the degree of diffusional control in isolated activation of hfX and bfII by extrinsic tenase and prothrombinase under flow conditions.** The absolution concentrations of hfXa (●) generated under flow conditions reported in Fig. 1 and bfIIa (○) generated under flow conditions (23) are shown as a function of the linear flow rate on a double logarithmic plot. A linear regression (*dotted line*) of the bfIIa data has a slope of −1.2 ± 0.1, indicative of a dilution-mediated model (Equation 3). A linear regression of the hfXa data has a slope of −0.68 ± 0.06, consistent with a diffusion-mediated model of activation under flow conditions (Equation 4).

studies and coincident studies with prothrombinase. This density of rTF(1–243) is above the critical TF surface density required for maximal fibrin and thrombin formation over a range of shear rates from 100 to 1000 s^{-1} as identified by Diamond and co-workers (15) and indicates that there is sufficient enzyme to support the application of the models of Laidler and co-workers (9–12). We assume this to be the surface density of extrinsic tenase because rTF(1–243) is the limiting component of the extrinsic tenase complex. This is approximately the same amount of surface-bound enzyme present in our studies of isolated bovine prothrombinase under flow (1.7 ± 0.9 fmol cm^{-2}) (23). In the current studies of hfII activation by surface-bound prothrombinase in coincidence with hfX activation by extrinsic tenase, we were unable to measure the density using our previously established methods (23) due to uncomplexed fXa remaining bound to the phospholipid membrane after rinsing with 100 capillary volumes at 100 s^{-1}. Because fVa is the limiting component in prothrombinase assembly, we assume that the density of prothrombinase is 1.8 fmol cm^{-2}, consistent with our previously published work (23).

Activation of hfX and hfII in Closed Systems—The activation of hfX by extrinsic tenase in a closed system was analyzed using a Michealis-Menten type analysis. The K_m and k_{cat} of the reaction at 37 °C were determined to be 1.2 ± 0.3 μM and 2 ± 0.2 s^{-1}, respectively, which is in good agreement with previously published values (39). The kinetic constants for the activation of hfII by prothrombinase in a closed system at 37 °C were determined to be 0.6 ± 0.3 μM and 35 ± 5 s^{-1}, respectively and are also in good agreement with previously published values (45, 46).

Activation of hfX under Flow—Absolute steady-state levels of hfXa are shown to decrease with increasing shear rate (Fig. 1); however, when corrected for average capillary passage time, the concentration of hfXa produced per unit time increases with shear rate (Fig. 1, *inset*). The difference between the generation of hfXa at the lowest shear rate (50 s^{-1}) and the two highest shear rates studied (500 and 1000 s^{-1}) per unit time is statistically significant. Similar observations have been reported previously by Gemmell *et al.* (47), which attributed the decrease in fXa generation at low shear rates to partial diffusional control due to substrate depletion in the catalytically active wall region.

To verify this finding, we employed the model of Laidler and co-workers (9, 10) as shown in Fig. 2. A double logarithmic plot of linear flow rate *versus* hfXa concentration has a slope of −0.68 ± 0.06, suggesting that the reaction is controlled by diffusion (Equation 4). Our previous results in the bovine prothrombinase system under flow (23) indicate that the activation of bfII is driven by dilution-mediated rather than diffusion-mediated control. When these data are shown as a double logarithmic plot of linear flow rate *versus* bfIIa concentration (Fig. 2), the slope is observed to be −1.2 ± 0.1, suggesting that the reaction is controlled by dilution-mediated processes (Equation 3), in agreement with our previous study (23). The activation of hfX, however, suggests that the effects of diffusional control cannot be neglected.

Coincident Activation of hfX and hfII with Preassembled Extrinsic Tenase and fVa under Flow—When hfII and hfX were flowed over PCPS-coated glass capillaries containing preassembled extrinsic tenase and hfVa, a decrease in the absolute concentrations of hfXa and hfIIa in the effluent with increasing shear rate was observed (Fig. 3, *A* and *B*). When hfXa generation is corrected for average capillary passage time (Fig. 3*A*, *inset*), differences in hfXa generation between shear rates are statistically significant ($p = 0.12$). Likewise, a similar trend was observed with the normalized thrombin generation profiles (Fig. 3*B*, *inset*) in which no statistical significance was also observed ($p = 0.55$), consistent with our previous studies of bfII activation by prothrombinase under flow conditions and a model of dilution-mediated activation across a physiologically relevant range of shear rates (23). Thus, in contrast to fX activation in isolation under flow conditions, the results of these coincident experiments suggest that fXa generation deviates from a model of pure diffusion-mediated control.

To further examine this hypothesis, the results of the coincident activation experiments were plotted as a double logarith-

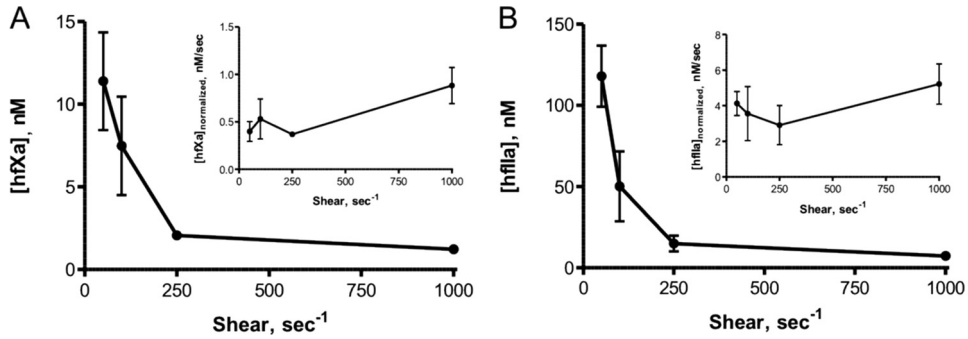

FIGURE 3. **Coincident activation of hfX and hfII by extrinsic tenase and prothrombinase under flow conditions.** hfX and hfII at physiologic plasma concentrations (170 nM and 1.4 μM, respectively) were flowed over a PCPS-coated glass capillary in which the extrinsic tenase and hfVa had been previously assembled. The effluent was collected dropwise and assayed for hfXa and hfIIa activity. *A*, absolute steady-state levels of hfXa ($n = 4$) are reported as well as mean ± S.D. (*error bars*) as a function of shear rate. Average capillary passage time-normalized levels of hfXa generation are shown in the *inset*. No statistically significant differences were observed. *B*, absolute steady-state levels of hfIIa ($n = 3$) are reported as well as mean ± S.D. as a function of shear rate. Average capillary passage time-normalized levels of hfIIa generation are shown in the *inset*. No statistically significant differences were observed.

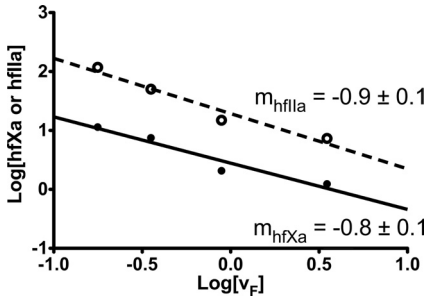

FIGURE 4. **Determination of the degree of diffusional control in the coincident activation of hfX and bfII by extrinsic tenase and prothrombinase under flow conditions.** The absolute concentrations of hfXa (●) generated under flow conditions reported in Fig. 3*A* and hfIIa (○) generated under flow conditions as reported in Fig. 3*B* are shown as a function of the linear flow rate on a double logarithmic plot. A linear regression (*dotted line*) of the bfIIa data has a slope of −0.9 ± 0.1, indicative of a dilution-mediated model (Equation 3). A linear regression of the hfXa data has a slope of −0.8 ± 0.1, suggesting that under these conditions, the activation of hfX deviates from a model of diffusion-mediated control (Equation 4).

mic plot of linear flow rate *versus* product concentration (Fig. 4). The slope of a linear regression fitted to the hfIIa generation data were −0.9 ± 0.1, consistent with Equation 3 and a model of dilution-mediated control. However, the slope of a linear regression of the hfXa generation data was −0.8 ± 0.1, which was decreased from that observed in the isolated system, suggesting that the activation of hfX in the coincident experiments deviates from a pure diffusion-mediated model (12). We hypothesized that this observed difference was the result of increased competition for membrane binding sites, which modulates the presentation of reaction product in the effluent.

Role of Binding Site Availability in Activation of hfX under Flow Conditions—To test the dependence of membrane binding of fX activation, we utilized two approaches. 1) We constructed a membrane with incorporated TF containing no PS, which eliminates the membrane's potential to interact with the γ-carboxyglutamate residues of fX. When the hfX (170 nM) was flowed over capillaries coated with a PC bilayer in which extrinsic tenase was preassembled at a shear rate of 100 s^{-1}, no detectable hfXa was observed in the effluent (data not shown). 2) In our second approach, we used b-Lac (K_d = 1.8 nM) to compete with fX and fXa for potential binding sites (48, 49). hfX (170 nM) was flowed over a PCPS-coated capillary (shear rate = 100 s^{-1}) containing extrinsic tenase and allowed to reach a steady state of hfXa generation before a solution containing hfX (170 nM) and b-Lac (25, 50, 100, and 200 nM) was introduced, and hfXa levels were measured for an additional ~780 s. As the concentration of b-Lac was increased, the percentage of hfXa activity measured in the effluent after ~780 s was observed to decrease (Fig. 5*A*), a pattern observed by Shi and Gilbert in test tube type experiments (49). The decrease in hfXa activity between 25 and 200 nM b-Lac was found to be statistically significant.

These data show that b-Lac effectively competes with hfX for binding sites under flow conditions, thereby inhibiting its activation. At the highest concentration of b-Lac studied (200 nM), the hfXa generation profile after the introduction of b-Lac showed two distinct regions, an increase in free hfXa followed by a rapid decrease in free hfXa levels (Fig. 5*B*). We attribute the initial increase in hfXa levels to be due to the release of bound hfXa as b-Lac initially competes for membrane binding sites. The following decrease in free hfXa is the result of b-Lac occupying potential hfX binding sites and inhibiting its efficient activation.

Binding of fII, fX, and fXa to a Phospholipid Membrane under Flow—Under steady-state conditions, the levels of bound substrates and products were estimated using the scheme proposed under "Theory." We treat the activation of fII to fIIa as occurring in a single step, ignoring the catalytically active intermediate meizothrombin, which is capable of membrane binding and indistinguishable from α-thrombin in the detection assay used in these studies. Using this approach and assuming that measured steady-state levels of fXa and fIIa are representative of unbound species restricted within a shear-dependent confined region, we estimate the percentage of occupied binding sites for three sets of conditions as shown in Table 3: isolated bovine prothrombinase (23), isolated human extrinsic tenase, and the coincident activation of hfII and hfX by prothrombinase and extrinsic tenase as described herein. In both the isolated and coincident experiments, fII occupies the greatest number of binding sites (38.9–72.2%), correspondent with its higher physiologic concentration and the fact that substrate depletion does not appear to be limiting to its activation under flow conditions. In isolated extrinsic tenase experiments, the

fraction of binding sites occupied by hfX decreases ~100-fold as the shear rate increases from 50 to 1000 s^{-1}, whereas the fraction of binding sites occupied by hfXa remains relatively constant (5.3–8.2%). This suggests that increased hfX binding at low shear rates may partially account for increased depletion of free hfX in the diffusion-limited region at lower shear rates and that the amount of hfX binding in these experiments is not sufficient to compete hfXa off of the membrane. In the coincident experiments, the percentage of binding sites occupied by hfII is at least 10-fold higher than those occupied by hfX and hfXa across the range of shear rates studied and is in good agreement with the bound bfII levels predicted in the isolated prothrombinase system. The fractions of binding sites occupied by hfX in the coincident system are also relatively constant (1.3–7.1%), whereas the percentage of binding sites occupied by hfXa is lower than those observed in the isolated system (1.9–3.8%). These results suggest that the introduction of hfII to the coincident system outcompetes hfXa for binding sites. The introduction of hfII to the hfX activation system also appears to regulate the number of binding sites occupied by hfX, making its presentation more consistent across the range of shear rates studied. Furthermore, by outcompeting hfXa for membrane binding sites, hfII regulates the amount of free hfXa in solution. Because fXa is a more potent enzyme when associated with an appropriate membrane, this may be a mechanism to regulate the activity of fXa under flow conditions (6).

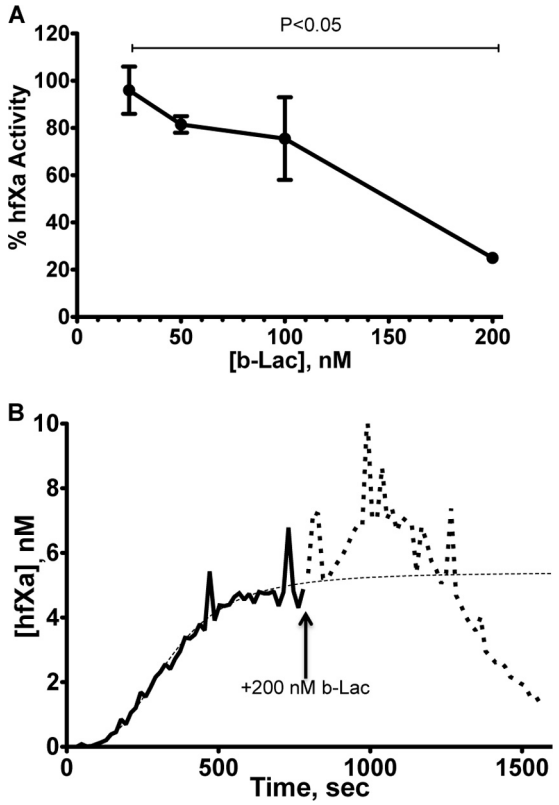

FIGURE 5. **Inhibition of extrinsic tenase activity by b-Lac under flow conditions.** PCPS-coated capillaries containing preassembled extrinsic tenase were perfused with a solution containing hfX (170 nM) at a shear rate of 100 s^{-1} for ~780 s to establish an initial steady-state level of hfXa generation after which the perfusate was switched to one containing hfX (170 nM) and b-Lac (25–200 nM) for an additional ~780 s. *A*, the percentage of hfXa activity in the effluent after perfusion with the b-Lac-containing solution is shown relative to the initial steady-state level of hfXa as a function of b-Lac concentration ($n = 2$). *B*, the average of two experiments with 200 nM b-Lac in the perfusate is shown. The *solid black line* shows hfXa generation with the primary perfusate containing only hfX, whereas the *dotted line* shows hfXa generation after the introduction of 200 nM b-Lac to the perfusate (as indicated by the *arrow*). The *thin dotted line* shows the fit of Equation 1 to the primary perfusate data. *Error bars*, S.D.

Modeling the Activations of fII and fX under Flow Conditions—The activations of fII and fX were modeled using the two kinetic schemes described under "Theory" (Equations 12 and 13) using appropriate kinetic constants (Table 4), and substrate concentrations (Table 5) and are illustrated in Fig. 6. The activation of bfII under flow conditions was modeled using our previously published data (23). Consistent with our previous work showing that the kinetics of bfII activation are independent of shear and not diffusion-limited, we found that bfIIa presentation was best modeled as activation of the total substrate within a shear-defined spatially confined region (Equation 12) and that modeling its activation using a membrane-localized model (Equation 13) overpredicts the observed levels of bfIIa (Fig. 6*A*). However, when free hfXa presentation was modeled using the bulk substrate model, the levels of hfXa were grossly underpredicted, whereas levels of free hfXa were more correctly modeled using the membrane-localized model (Fig. 6*B*). This further suggests that the ability of hfX to bind to the membrane under flow conditions is critical to its effective activation, consistent with previous studies (2, 27, 28, 31). When these modeling schemes were applied to our coincident activation experiments (Fig. 4, *C* and *D*), the observed results were similar to those in the isolated systems, suggesting that under this set of conditions, the same regimes are still applicable and that at physiologic plasma concentration, the ability of hfX to bind to an appropriate phospholipid membrane is critical to its activation.

TABLE 4
Kinetic constants

Species	K_m	k_{cat}
	μM	s^{-1}
Bovine prothrombinase (flow, 250 s^{-1}) (23)	0.16	27
Human prothrombinase	0.6	35
Human extrinsic tenase	1.2	2

TABLE 3
Percentage of binding sites occupied

Shear	Isolated prothrombinase, bfII	Isolated extrinsic tenase			Coincident experiments			
		hfX	hfXa	Total	hfII	hfX	hfXa	Total
s^{-1}	%	%	%	%	%	%	%	%
50		10.4	8.2	12.9	69.2	7.1	2.9	79.2
100	72.2	6.1	8.5	14.6	67.1	6.2	3.1	67.4
250	63.3	2.9	7.1	10	60.2	5.9	1.8	67.9
1000	38.9	0.1	5.3	5.4	39.0	1.3	3.8	40.4

TABLE 5

Calculated steady-state concentrations of free and bound fII and fX

Concentrations are reported within the shear-defined r.m.s. diffusion distance-defined volume element.

Shear	Isolated prothrombinase (23)		Isolated extrinsic tenase		Coincident experiments			
	$[bfII]_f$	$[bfII]_b$	$[hfX]_f$	$[hfX]_b$	$[hfII]_f$	$[hfII]_b$	$[hfX]_f$	$[hfX]_b$
s^{-1}	nM	nM	nM	nM	nM	nM	nM	nM
50			32.0	71.0	764	472	85.8	48.7
100	597	696	17.7	58.4	654	647	65.7	59.9
250	396	967	8.2	45.1	432	921	45.8	90.0
1000	146	1189	0.2	2.5	161	1193	5.8	40.0

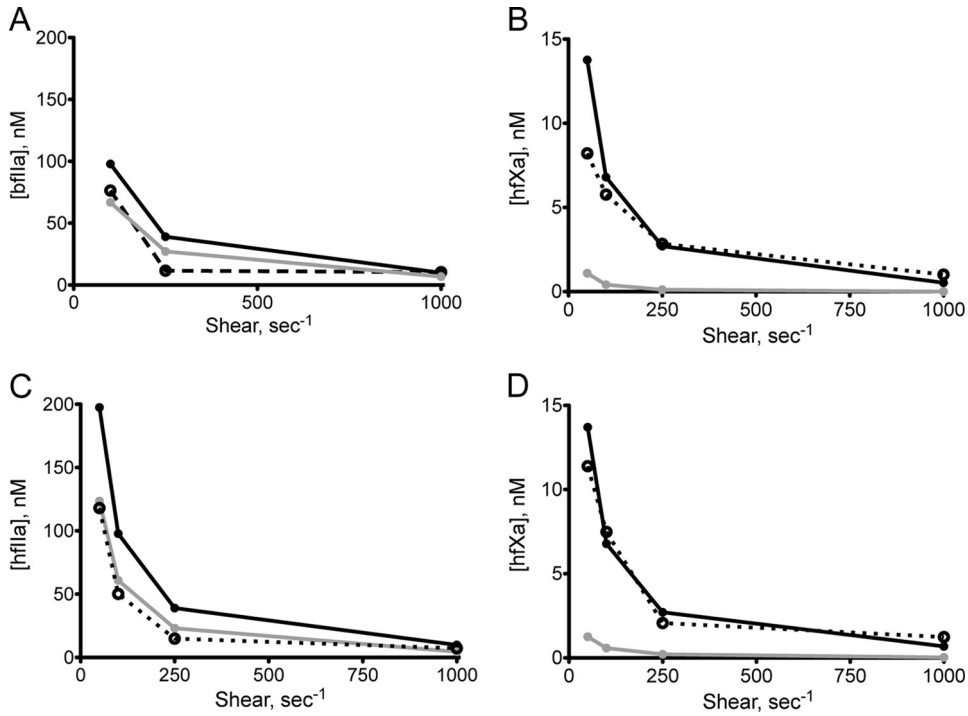

FIGURE 6. **Models of fIIa and fXa generation.** fIIa and fXa generation under steady-state conditions were modeled using the bulk substrate diffusion model (Equation 12; *gray line*) and membrane-localized model (Equation 13; *black line*). Experimental data are shown with a *dotted line*. *A*, isolated bovine prothrombinase (23); *B*, isolated extrinsic tenase; *C*, coincident activation of hfII; *D*, coincident activation of hfX.

TABLE 6

Steady-state concentrations of free and bound products (fIIa and fXa)

Concentrations are reported within the shear-defined r.m.s. diffusion distance-defined volume element.

Shear	Isolated prothrombinase (23), $[bfIIa]^a$	Isolated extrinsic tenase		Coincident experiments		
		$[hfXa]_f^a$	$[hfXa]_b^b$	$[hfIIa]^a$	$[hfXa]_f^a$	$[hfXa]_b^b$
s^{-1}	nM	nM	nM	nM	nM	nM
50		11.4	55.6	164	15.8	19.7
100	107	11.4	82.4	99.3	14.8	29.6
250	36.4	8.9	107.8	46.8	6.5	28.0
1000	65.3	6.3	161.0	45.9	7.8	116.5

[a] Empirical value.
[b] Calculated value.

Local Steady-state Concentrations of Activated Products—Using the r.m.s. diffusion distance spatial confinement and dissociative equilibrium scheme outlined under "Theory," we determined the amount of spatially confined fIIa and fXa (free and bound) that could be expected within these regions (Table 6). fIIa and free fXa levels are those determined from experimental results multiplied by the appropriate shear-dependent spatial confinement factor. Bound fXa levels are those predicted by our equilibrium dissociation model. Using this model, spatially confined fIIa levels are well above the critical concentration of 2 nM required for fibrin plug formation (50). In both the isolated and coincident models of hfX activation, the concentrations of bound hfXa are significantly higher than those of the free species; however, in the coincident model, the levels of bound hfXa are more comparable with those of free hfXa except at the highest shear rate studied (1000 s^{-1}). We attribute this pattern to competition with hfII for available binding sites, leading to a decrease in bound hfXa. At 1000 s^{-1}, fewer binding sites are occupied by hfII (Table 3), leading to a relative increase in bound hfXa.

DISCUSSION

The activation of fX under physiologically relevant flow conditions, as reported previously by Nemerson and co-workers (27, 51), is subject to diffusion-mediated control. In this study, we confirm this finding by observing that when a physiologic concentration of fX (170 nM) is flowed over the capillary at low shear rates (50–100 s^{-1}), the average flow rate-normalized fXa levels in the effluent are decreased from those at higher shear rates, indicating substrate depletion in the catalytically active wall region. This is in contrast to the isolated prothrombinase system under flow reported previously, in which no shear dependence is observed in the normalized levels of bfIIa generated at steady state, indicating that this system is regulated purely by dilution-mediated control across a range of physiologically relevant shear rates (23). These contrasting findings support the concept that coagulation throughout the vasculature is subject to regulation by local shear conditions that are specific to different membrane-localized enzyme complexes (extrinsic tenase *versus* prothrombinase). Furthermore, results from the current study show that when hfX and hfII are activated coincident with each other by extrinsic tenase and prothrombinase, respectively, hfX activation appears to deviate from a diffusion-mediated system. This suggests that in more complex membrane-dependent systems, there is an additional regulating component of the coagulation process under flow conditions.

To explain this observation, we developed models of fII and fX activation under steady-state flow conditions. The results of these models suggest that whereas the activation of fII can be modeled using its steady-state concentration in the bulk fluid, the activation of fX is best modeled using the membrane-bound population of fX. Previous studies have shown that fX binding to the membrane is the rate-limiting step in its activation under flow (52) and that furthermore the active enzyme fXa can compete with fX for membrane binding sites, resulting in product inhibition (31). In this study, we show that at low shear rates, fX and fXa compete with fII for membrane binding sites under flow, resulting in a mechanism that mitigates diffusion's role in regulating fX activation. Combined, these observations promote a model in which coagulation factors may compete with each other under flow conditions to regulate the process of blood coagulation under flow.

This conclusion is not unexpected because others have previously noted the importance of the vessel dimension and vessel wall composition in affecting the efficiency of surface-dependent enzyme complexes (18, 53). TF density has been shown to have significant thresholding effects under flow conditions in both empirical (15) and computational models (19, 22) for fibrin clot formation. Furthermore, shear rates have also been shown to have similar thresholding effects (18), with fibrin clot formation impaired at increasing shear rates. A role for the surface in the coagulation process under flow has also been suggested previously (18, 53). Runyon *et al.* (18), in addition to previous work by Esmon and Owen (53), also note that in vessels with a small volume/surface ratio, the surface-bound inhibitor thrombomodulin can regulate clot propagation, whereas in vessels with a large volume/surface area ratio, clot propagation is mostly regulated by shear-induced dilution effects. We propose that under conditions where surface inhibition of clot propagation is insufficient, competition for membrane binding sites may regulate the amount of procoagulant enzymes at the site of thrombus formation and consequently self-limit thrombus growth.

Acknowledgments—We thank Ruhin Yuridullah and Dr. Jolanta Amblo for assisting in immunoassays for TF quantification and Dr. Thomas Orfeo for helpful discussions and assistance in preparing the manuscript.

REFERENCES

1. Mann, K. G., Nesheim, M. E., Church, W. R., Haley, P., and Krishnaswamy, S. (1990) Surface-dependent reactions of the vitamin K-dependent enzyme complexes. *Blood* **76,** 1–16
2. Krishnaswamy, S. (1992) The interaction of human factor VIIa with tissue factor. *J. Biol. Chem.* **267,** 23696–23706
3. Silverberg, S. A., Nemerson, Y., and Zur, M. (1977) Kinetics of the activation of bovine coagulation factor X by components of the extrinsic pathway. Kinetic behavior of two-chain factor VII in the presence and absence of tissue factor. *J. Biol. Chem.* **252,** 8481–8488
4. Butenas, S., Brummel, K. E., Bouchard, B. A., and Mann, K. G. (2003) How factor VIIa works in hemophilia. *J. Thromb. Haemost.* **1,** 1158–1160
5. Butenas, S., Brummel, K. E., Paradis, S. G., and Mann, K. G. (2003) Influence of factor VIIa and phospholipids on coagulation in "acquired" hemophilia. *Arterioscler. Thromb. Vasc. Biol.* **23,** 123–129
6. Nesheim, M. E., Taswell, J. B., and Mann, K. G. (1979) The contribution of bovine factor V and factor Va to the activity of prothrombinase. *J. Biol. Chem.* **254,** 10952–10962
7. Nesheim, M. E., Tracy, R. P., and Mann, K. G. (1984) "Clotspeed," a mathematical simulation of the functional properties of prothrombinase. *J. Biol. Chem.* **259,** 1447–1453
8. Krishnaswamy, S., Jones, K. C., and Mann, K. G. (1988) Prothrombinase complex assembly. Kinetic mechanism of enzyme assembly on phospholipid vesicles. *J. Biol. Chem.* **263,** 3823–3834
9. Laidler, K. J., and Bunting, P. S. (1980) The kinetics of immobilized enzyme systems. *Methods Enzymol.* **64,** 227–248
10. Koyayashi, T., and Laidler, K. J. (1974) Theory of the kinetics of reactions catalyzed by enzymes attached to the interior surfaces of tubes. *Biotechnol. Bioeng.* **16,** 99–118
11. Kobayashi, T., and Laidler, K. J. (1974) Theory of the kinetics of reactions catalyzed by enzymes attached to membranes. *Biotechnol. Bioeng.* **16,** 77–97
12. Bunting, P. S., and Laidler, K. J. (1974) Flow kinetics of L-asparaginase attached to nylon tubing. *Biotechnol. Bioeng.* **16,** 119–134
13. Hathcock, J. J. (2006) Flow effects on coagulation and thrombosis. *Arterioscler. Thromb. Vasc. Biol.* **26,** 1729–1737
14. Diamond, S. L. (2010) Tissue factor activity under flow. *Thromb. Res.* **125,** Suppl. 1, S29–S30
15. Okorie, U. M., Denney, W. S., Chatterjee, M. S., Neeves, K. B., and Diamond, S. L. (2008) Determination of surface tissue factor thresholds that trigger coagulation at venous and arterial shear rates. Amplification of 100 fM circulating tissue factor requires flow. *Blood* **111,** 3507–3513
16. Kastrup, C. J., Shen, F., Runyon, M. K., and Ismagilov, R. F. (2007) Characterization of the threshold response of initiation of blood clotting to stimulus patch size. *Biophys. J.* **93,** 2969–2977
17. Shen, F., Kastrup, C. J., Liu, Y., and Ismagilov, R. F. (2008) Threshold response of initiation of blood coagulation by tissue factor in patterned microfluidic capillaries is controlled by shear rate. *Arterioscler. Thromb. Vasc. Biol.* **28,** 2035–2041
18. Runyon, M. K., Kastrup, C. J., Johnson-Kerner, B. L., Ha, T. G., and Ismagilov, R. F. (2008) Effects of shear rate on propagation of blood clotting determined using microfluidics and numerical simulations. *J. Am. Chem. Soc.* **130,** 3458–3464

19. Jordan, S. W., and Chaikof, E. L. (2011) Simulated surface-induced thrombin generation in a flow field. *Biophys. J.* **101,** 276–286
20. Leiderman, K., and Fogelson, A. L. (2011) Grow with the flow. A spatial-temporal model of platelet deposition and blood coagulation under flow. *Math. Med. Biol.* **28,** 47–84
21. Fogelson, A. L., and Tania, N. (2005) Coagulation under flow. The influence of flow-mediated transport on the initiation and inhibition of coagulation. *Pathophysiol. Haemost. Thromb.* **34,** 91–108
22. Kuharsky, A. L., and Fogelson, A. L. (2001) Surface-mediated control of blood coagulation. The role of binding site densities and platelet deposition. *Biophys. J.* **80,** 1050–1074
23. Haynes, L. M., Dubief, Y. C., Orfeo, T., and Mann, K. G. (2011) Dilutional control of prothrombin activation at physiologically relevant shear rates. *Biophys. J.* **100,** 765–773
24. Schoen, P., Lindhout, T., Willems, G., and Hemker, H. C. (1990) Continuous flow and the prothrombinase-catalyzed activation of prothrombin. *Thromb. Haemost.* **64,** 542–547
25. Billy, D., Speijer, H., Willems, G., Hemker, H. C., and Lindhout, T. (1995) Prothrombin activation by prothrombinase in a tubular flow reactor. *J. Biol. Chem.* **270,** 1029–1034
26. Schoen, P., and Lindhout, T. (1991) Flow and the inhibition of prothrombinase by antithrombin III and heparin. *Blood* **78,** 118–124
27. Contino, P. B., Andree, H. A., and Nemerson, Y. (1994) Flow dependence of factor X activation by tissue factor-factor VIIa. *J. Physiol Pharmacol.* **45,** 81–90
28. Krishnaswamy, S., Field, K. A., Edgington, T. S., Morrissey, J. H., and Mann, K. G. (1992) Role of the membrane surface in the activation of human coagulation factor X. *J. Biol. Chem.* **267,** 26110–26120
29. Butenas, S., Dee, J. D., and Mann, K. G. (2003) The function of factor XI in tissue factor-initiated thrombin generation. *J. Thromb. Haemost.* **1,** 2103–2111
30. Hathcock, J. J., Rusinova, E., Gentry, R. D., Andree, H., and Nemerson, Y. (2005) Phospholipid regulates the activation of factor X by tissue factor/factor VIIa (TF/VIIa) via substrate and product interactions. *Biochemistry* **44,** 8187–8197
31. Hathcock, J., Rusinova, E., Vaananen, H., and Nemerson, Y. (2007) Lipid-bound factor Xa regulates tissue factor activity. *Biochemistry* **46,** 6134–6140
32. Higgins, D. L., and Mann, K. G. (1983) The interaction of bovine factor V and factor V-derived peptides with phospholipid vesicles. *J. Biol. Chem.* **258,** 6503–6508
33. Katzmann, J. A., Nesheim, M. E., Hibbard, L. S., and Mann, K. G. (1981) Isolation of functional human coagulation factor V by using a hybridoma antibody. *Proc. Natl. Acad. Sci. U.S.A.* **78,** 162–166
34. Bajaj, S. P., and Mann, K. G. (1973) Simultaneous purification of bovine prothrombin and factor X. Activation of prothrombin by trypsin-activated factor X. *J. Biol. Chem.* **248,** 7729–7741
35. Broze, G. J., Jr., Girard, T. J., and Novotny, W. F. (1990) Regulation of coagulation by a multivalent Kunitz-type inhibitor. *Biochemistry* **29,** 7539–7546
36. Lundblad, R. L., Kingdon, H. S., and Mann, K. G. (1976) Thrombin. *Methods Enzymol.* **45,** 156–176
37. Kalb, E., Frey, S., and Tamm, L. K. (1992) Formation of supported planar bilayers by fusion of vesicles to supported phospholipid monolayers. *Biochim. Biophys. Acta* **1103,** 307–316
38. Tamm, L. K., and McConnell, H. M. (1985) Supported phospholipid bilayers. *Biophys. J.* **47,** 105–113
39. Krudysz-Amblo, J., Jennings, M. E., 2nd, Mann, K. G., and Butenas, S. (2010) Carbohydrates and activity of natural and recombinant tissue factor. *J. Biol. Chem.* **285,** 3371–3382
40. Parhami-Seren, B., Butenas, S., Krudysz-Amblo, J., and Mann, K. G. (2006) Immunologic quantitation of tissue factors. *J. Thromb. Haemost.* **4,** 1747–1755
41. Marsh, D. (1996) Intrinsic curvature in normal and inverted lipid structures and in membranes. *Biophys. J.* **70,** 2248–2255
42. Shaw, A. W., Pureza, V. S., Sligar, S. G., and Morrissey, J. H. (2007) The local phospholipid environment modulates the activation of blood clotting. *J. Biol. Chem.* **282,** 6556–6563
43. Kung, C., Hayes, E., and Mann, K. G. (1994) A membrane-mediated catalytic event in prothrombin activation. *J. Biol. Chem.* **269,** 25838–25848
44. Nesheim, M. E., Eid, S., and Mann, K. G. (1981) Assembly of the prothrombinase complex in the absence of prothrombin. *J. Biol. Chem.* **256,** 9874–9882
45. Orfeo, T., Brufatto, N., Nesheim, M. E., Xu, H., Butenas, S., and Mann, K. G. (2004) The factor V activation paradox. *J. Biol. Chem.* **279,** 19580–19591
46. Rosing, J., Tans, G., Govers-Riemslag, J. W., Zwaal, R. F., and Hemker, H. C. (1980) The role of phospholipids and factor Va in the prothrombinase complex. *J. Biol. Chem.* **255,** 274–283
47. Gemmell, C. H., Nemerson, Y., and Turitto, V. (1990) The effects of shear rate on the enzymatic activity of the tissue factor-factor VIIa complex. *Microvasc. Res.* **40,** 327–340
48. Andersen, M. H., Graversen, H., Fedosov, S. N., Petersen, T. E., and Rasmussen, J. T. (2000) Functional analyses of two cellular binding domains of bovine lactadherin. *Biochemistry* **39,** 6200–6206
49. Shi, J., and Gilbert, G. E. (2003) Lactadherin inhibits enzyme complexes of blood coagulation by competing for phospholipid-binding sites. *Blood* **101,** 2628–2636
50. Brummel, K. E., Paradis, S. G., Butenas, S., and Mann, K. G. (2002) Thrombin functions during tissue factor-induced blood coagulation. *Blood* **100,** 148–152
51. Gemmell, C. H., Turitto, V. T., and Nemerson, Y. (1988) Flow as a regulator of the activation of factor X by tissue factor. *Blood* **72,** 1404–1406
52. McGee, M. P., Li, L. C., and Xiong, H. (1992) Diffusion control in blood coagulation. Activation of factor X by factors IXa/VIIIa assembled on human monocyte membranes. *J. Biol. Chem.* **267,** 24333–24339
53. Esmon, C. T., and Owen, W. G. (1981) Identification of an endothelial cell cofactor for thrombin-catalyzed activation of protein C. *Proc. Natl. Acad. Sci. U.S.A.* **78,** 2249–2252
54. Bloom, J. W., Nesheim, M. E., and Mann, K. G. (1979) Phospholipid-binding properties of bovine factor V and factor Va. *Biochemistry* **18,** 4419–4425
55. Lanchantin, G. F., Friedmann, J. A., DeGroot, J., and Mehl, J. W. (1963) Preparation of human plasma prothrombin and some of its sedimentation properties. *J. Biol. Chem.* **238,** 238–243
56. Jackson, C. M., and Hanahan, D. J. (1968) Studies on bovine factor X. II. Characterization of purified factor X. Observations on some alterations in zone electrophoretic and chromatographic behavior occurring during purification. *Biochemistry* **7,** 4506–4517
57. Radcliffe, R. D., and Barton, P. G. (1972) The purification and properties of activated factor X. Bovine factor X activated with Russell's viper venom. *J. Biol. Chem.* **247,** 7735–7742
58. Haynes, L. M., Dubief, Y. C., and Mann, K. G. (2011) The presentations of factor Xa and thrombin under flow. *J. Thromb. Haemost.* **9,** 346